The Magnetic Properties of Three Copper(II) Trichloroacetate Adducts with Caffeine and the Crystal Structure of Dicaffeinetetrakis(μ-trichloroacetato)dicopper(II) Dibenzene Solvate, $[Cu(CCl_3COO)_2(C_8H_{10}N_4O_2)]_2 \cdot 2C_6H_6$

Hiroshi Horie,[a] Steinar Husebye,[b,c] Michinobu Kato,[d] Edward A. Meyers,[b] Yoneichiro Muto,[a] I. Suzuki,[e] Tadashi Tokii[a] and Ralph A. Zingaro[b]

[a]Department of Chemistry, Faculty of Science and Engineering, Saga University, Saga 840, Japan, [b]Department of Chemistry, Texas A&M University, College Station, TX 77843, USA, [c]Department of Chemistry, University of Bergen, 5000 Bergen, Norway, [d]Department of Chemistry, Aichi Prefectural University, Mizuho-ku, Nagoya 467 and [e]Department of Electrical and Computer Engineering, Nagoya Institute of Technology, Showa-ku, Nagoya 466, Japan

Horie, H., Husebye, S., Kato, M., Meyers, E. A., Muto, Y., Suzuki, I., Tokii, T. and Zingaro, R. A., 1986. The Magnetic Properties of Three Copper(II) Trichloroacetate Adducts with Caffeine and the Crystal Structure of Dicaffeinetetrakis(μ-trichloroacetato)dicopper(II) Dibenzene Solvate, $[Cu(CCl_3COO)_2(C_8H_{10}N_4O_2)]_2 \cdot 2C_6H_6$. – Acta Chem. Scand. A 40: 579–589.

Three copper(II) trichloroacetate adducts with caffeine have been prepared: $[Cu(CCl_3COO)_2(caf)]_2 \cdot 2C_6H_6$ (*1*), $[Cu(CCl_3COO)_2(caf)]_2$, light green form, (*2*) and a pale green form, (*3*). All three adducts display a dimer type of antiferromagnetism. Compounds (*2*) and (*3*) are magnetically different and (*1*) and (*2*) undergo changes in magnetic properties at ca. 200 K, indicating phase changes. The structure of (*1*) was solved at room temperature. An attempt to solve the low temperature structure had to be abandoned due to cracking of the crystals upon cooling. The dark green crystals of (*1*) had the following properties: M_r = 1012.53, monoclinic, *C2/m*; a = 20.045(6), b = 13.715(3), c = 10.794(2) Å; β = 119.01(2)°, V = 2592.1 Å^3, Z = 2, D_x = 1.253 g cm^{-3}. λ(Cu$K\alpha$) = 1.54184 Å, μ = 72.5 cm^{-1}, $F(000)$ = 1324, T = 296 K, final R = 0.068 for 1888 unique, observed reflections. The complex has the structure usually found in dimeric copper carboxylates of the type $[Cu(RCOO)_2L]_2$, each copper atom in the centrosymmetric dimers having distorted square pyramidal symmetry with N9 of the caffeine molecule in the apical position and relatively long Cu–Cu distances of 2.852(1) Å. The Cu–O bond lengths average 1.973 Å, Cu–N9 = 2.121(5) Å and the angle Cu---Cu–N9 is 163.4 (2)°. A singlet-triplet energy separation, $-2J$, of only 194.5 cm^{-1} was found. The EPR spectrum at room temperature of (*3*) differed from the spectra of (*1*) and (*2*), possibly indicating trigonal bipyramidal coordination to Cu(II). However, after the phase change at low temperature, (*1*) displays a similar spectrum.

The recent structural studies on dimeric copper(II) carboxylate adducts, $[Cu(RCOO)_2L]_2$, have demonstrated that the metal–metal distance becomes longer as either the acidity of the parent carboxylic acid, RCOOH,[1] or the basicity of the axial ligand, L,[2] becomes greater. A greater Cu–Cu distance is usually associated with a larger displacement of the copper(II) ions from the equatorial plane containing four oxygen atoms. Consequently, the variations of both the group R and the ligand L affect the strength of the Cu–O bonds in the CuO_4 basal plane with an accompanying deformation of the bridging framework. In thirteen dimeric copper(II) acetate adducts, the Cu–Cu distances (2.581–2.671 Å)[2] span a range of 0.09 Å. On the other hand, the Cu–Cu distances found for dimeric copper(II) trichloroacetate adducts, $[Cu(CCl_3COO)_2L]_2$, vary quite con-

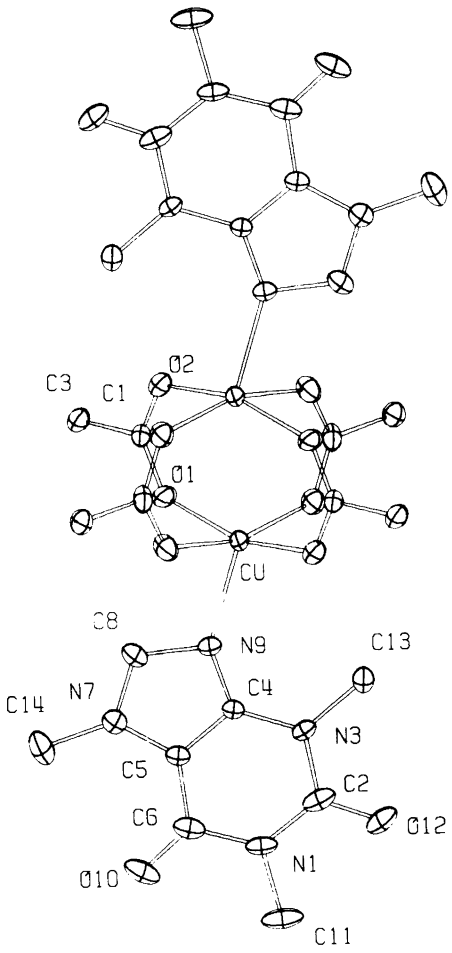

Fig. 1. The structure of the dimer, (*1*).

siderably: 2.731 Å for L = benzonitrile,[3] 2.776 Å for L = 2-chloropyridine,[1] and 3.256 Å for L = 2,2,6,6,-tetramethylpiperidinyl-1-oxy.[4] These structural data indicate that the flexibility of the bridging trichloroacetate ligand is quite great.

Table 1. Positional parameters and their estimated standard deviations.[a]

Atom	*x*	*y*	*z*
Cu	0.6923(5)	0	0.13171(9)
Cl 1	0.1258(6)	0.2995(5)	−0.0351(9)
Cl 2	0.0281(4)	0.2449(9)	−0.3211(7)
Cl 3	0.1623(4)	0.1429(9)	−0.1588(10)
O1	0.0903(2)	0.1008(3)	0.0229(3)
O2	−0.0170(2)	0.0998(3)	−0.1831(3)
C1	0.0492(3)	0.1262(4)	−0.0989(5)
C3	0.0859(2)	0.2021(4)	−0.1550(4)
O10	0.4412(3)	0	0.6233(7)
O12	0.2650(4)	0	0.7745(5)
N1	0.3528(3)	0	0.6982(6)
N3	0.2186(3)	0	0.5352(5)
N7	0.3106(3)	0	0.3270(6)
N9	0.1861(3)	0	0.2879(5)
C2	0.2782(5)	0	0.6748(7)
C4	0.2358(4)	0	0.4259(6)
C5	0.3099(4)	0	0.4523(7)
C6	0.3741(4)	0	0.5934(8)
C8	0.2346(4)	0	0.2274(8)
C11	0.4122(6)	0	0.8497(8)
C13	0.1380(4)	0	0.5040(8)
C14	0.3747(5)	0	0.3008(11)
C15	0.2462(5)	0.2463(5)	0.3669(8)
C16	0.3171(4)	0.2449(5)	0.4906(8)
C17	0.1793(4)	0.2496(5)	0.3756(7)

[a]Only the set of chlorines with occupancy = 0.50 is included.

Dimeric copper(II) trichloroacetate adducts may therefore be a suitable choice for a study of the structural factors influencing magnetic properties.

In the course of our studies of dimeric copper(II) trichloroacetate adducts, we prepared two magnetically different modifications of the caffeine adduct, $[Cu(CCl_3COO)_2(caf)]_2$, one light green, (*2*), and the other pale green, (*3*). A com-

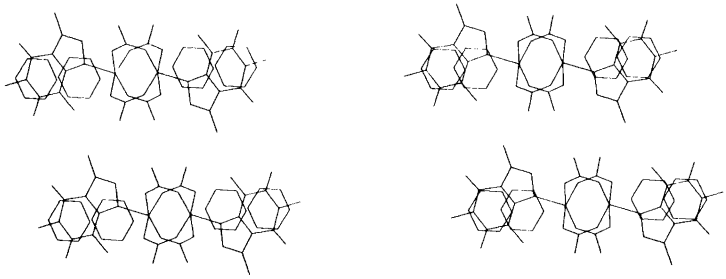

Fig. 2. Stereoview of the dimer $[Cu(CCl_3COO)_2(caf)]_2 \cdot (2bz)$, (*1*).

Table 2. Interatomic distances (Å) and angles (°) with e.s.d.s in parentheses.[a]

Cu–Cu′	2.852(2)	O1–Cu–O1*	88.1(2)
Cu–O1	1.987(4)	O1–Cu–O2*	88.7(2)
Cu′–O2	1.959(4)	O2′–Cu–O2*	88.6(2)
C1–O1	1.215(5)	O1–Cu–O2′	161.6(1)
C1–O2	1.245(5)	O1–Cu–N9	90.0(2)
C1–C3	1.556(8)	O2–Cu′–N9′	108.1(2)
C3–Cl1	1.760(9)	O1–C1–O2	129.0(6)
C3–Cl2	1.699(8)	Cu–O1–C1	127.7(4)
C3–Cl3	1.751(12)	Cu′–O2–C1	121.6(4)
Cu–N9	2.121(5)	O1–C1–C3	114.4(4)
N1–C2	1.391(12)	O2–C1–C3	116.6(4)
C2–N3	1.397(7)	O1–Cu–Cu′	78.1(2)
N3–C4	1.379(11)	O2–Cu′–Cu	83.5(2)
C4–C5	1.370(11)	N9–Cu–Cu′	163.4(3)
C5–C6	1.441(8)	Cu–N9–C4	145.9(6)
C6–N1	1.390(13)	Cu–N9–C8	112.1(4)
C5–N7	1.359(11)	C4–N9–C8	102.0(6)
N7–C8	1.373(8)	C6–N1–C2	125.5(5)
C8–N9	1.411(12)	C6–N1–C11	119.8(7)
N9–C4	1.331(7)	C11–N1–C2	114.7(8)
C6–O10	1.221(10)	N1–C2–N3	118.5(8)
N1–C11	1.485(9)	N1–C2–O12	120.8(6)
C2–O12	1.227(12)	O12–C2–N3	120.7(9)
N3–C13	1.482(11)	C2–N3–C4	119.0(7)
N7–C14	1.444(15)	C2–N3–C13	120.9(7)
C15–C16	1.401(9)	C13–N3–C4	120.2(5)
C15–C17	1.388(13)	N3–C4–C5	121.1(5)
C17–C16′	1.412(12)	N3–C4–N9	126.5(6)
C3–Cl4	1.870(11)	N9–C4–C5	112.3(7)
C3–Cl5	1.592(10)	C4–C5–C6	122.9(8)
C3–Cl6	1.717(12)	C4–C5–N7	109.1(5)
C3–Cl7	1.744(17)	C6–C5–N7	128.0(8)
C3–Cl8	1.780(16)	C5–C6–N1	112.9(7)
C3–Cl9	1.722(28)	C5–C6–O10	125.8(9)
		O10–C6–N1	121.3(6)
		C5–N7–C8	103.7(7)
		C5–N7–C14	129.4(6)
		C14–N7–C8	126.9(8)
		N7–C8–N9	112.9(7)
		C16–C15–C17	120.1(8)
		C15–C17–C16′	119.9(6)
		C17′–C16–C15	120.0(8)
		C1–C3–Cl1	110.7(5)
		C1–C3–Cl2	115.6(4)
		C1–C3–Cl3	106.4(5)
		Cl1–C3–Cl2	110.3(5)
		Cl1–C3–Cl3	106.2(5)
		Cl2–C3–Cl3	107.0(6)

[a] Primed atoms are related to atoms in the asymmetric unit (Table 1) by the molecular centre of symmetry. Atoms marked # are likewise related by the molecular mirror plane to those of Table 1 and by the molecular centre of symmetry to the starred (*) atoms.

Table 3. Best planes in the dimer.

No. of plane	Atoms in plane	Δ maximum[a] (Å)	Dist. of other atoms from plane (Å)
1[b]	Caffeine, Cu	0	
2	C1, O1, O2	0	C3: 0.005; Cu: 0.110; Cu′: 0.082
3	O1, O1*, O2*, O2′ (basal plane)	0	Cu: 0.316; N: 2.385
4	O1, O2, O1′, O2′, Cu, Cu′	0.008	
5	Benzene ring	0.009	
		Interplanar angles (°)	
	1–2: 137.8	1–4: 135.0	2–4: 2.8
	1–3: 90	1–5: 2.9	

[a]Maximum devn. of constituent atoms from plane. [b]Crystallographic mirror plane.

plex $[Cu(CCl_3COO)_2(caf)]_2 \cdot (2bz)$, (*1*), where bz = benzene, was also isolated. These three complexes all display a dimer type of antiferromagnetism. For both (*1*) and (*2*) a change in magnetic properties at ca. 200 K is observed, indicating a phase transition. Hence, the crystal structure of the benzene adduct was determined by X-ray diffraction in order to clarify the structure and to the magnetic properties in more detail in relation to the structure.

Experimental

Syntheses. $[Cu(CCl_3COO)_2(caf)]_2 \cdot (2bz)$, (*1*): A solution of caffeine (1 mmol) in benzene (20 ml)

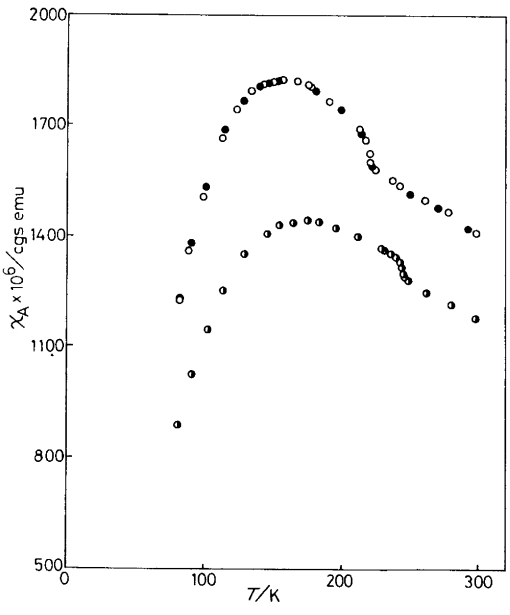

Fig. 3. Variation of magnetic susceptibilities with temperature. (○) Sample A and (●) B of the light green form of $[Cu(CCl_3COO)_2(caf)]_2$, (*2*); (◑) $[Cu(CCl_3COO)_2(caf)]_2 \cdot (2bz)$, (*1*).

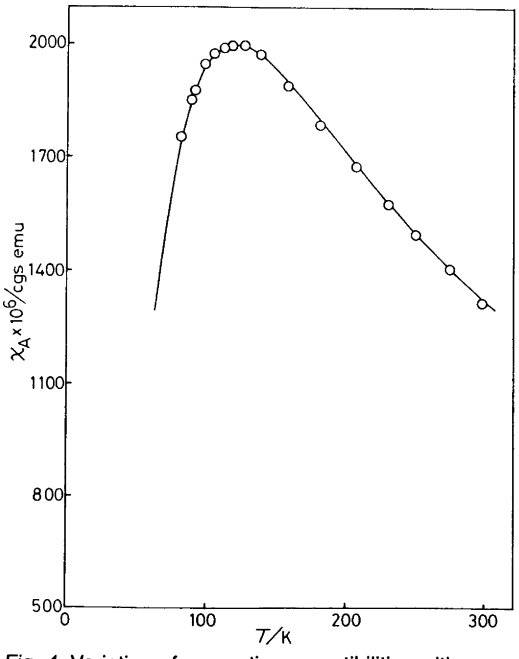

Fig. 4. Variation of magnetic susceptibilities with temperature. (○) Pale green form of $[Cu(CCl_3COO)_2(caf)]_2$, (*3*). Solid line shows calculated susceptibilities.

Table 4. Magnetic susceptibilities[a] for $[Cu(CCl_3COO)_2(caf)]_2$, light green form, (*2*). $\chi_{dia} = -272\times10^{-6}$ cgs emu.

Sample A		Sample B	
T/K	$10^6\,\chi_A$	*T*/K	$10^6\,\chi_A$
Low temp. region		Low temp. region	
81.3	1225	81.4	1228
88.3	1359	90.1	1383
98.1	1507	100.0	1540
112.1	1667	114.8	1689
123.4	1748	128.1	1773
133.6	1801	139.9	1807
143.2	1817	146.2	1817
150.3	1826	153.9	1822
156.8	1824	178.3	1793
166.4	1821	198.3	1745
176.1	1807		
177.6	1803	Intermediate temp. region	
190.9	1771	214.2	1680
212.6	1696	221.2	1590
Intermediate temp. region		High temp. region	
216.0	1680	250.3	1519
217.0	1659	270.2	1476
220.1	1626	292.0	1416
221.8	1600		
224.3	1582		
High temp. region			
237.5	1555		
243.4	1542		
260.0	1508		
260.6	1505		
278.1	1473		
298.0	1414		

[a]Magnetic susceptibilities (χ_A) and diamagnetic corrections (χ_{dia}) are given in cgs emu mol^{-1} (1 cgs emu $mol^{-1} = 4\pi\ 10^{-6}\ m^3\ mol^{-1}$).

was added to a solution of $Cu(CCl_3COO)_2\cdot 3H_2O$ (1 mmol) in benzene (20 ml) and 2,2-dimethoxypropane (1 ml). The greenish-brown precipitate which formed after a few min was filtered off and the product recrystallized by adding benzene slowly to an acetonitrile solution of the complex. After washing with petroleum ether, the crystals were dried *in vacuo* at room temperature. Anal. $C_{18}H_{16}N_4O_6Cl_6Cu$: C, H, N, Cu.

$[Cu(CCl_3COO)_2(caf)]_2$ (light green form), (*2*): This compound was prepared in the same way as above, using toluene instead of benzene. Anal. $C_{12}H_{10}N_4O_6Cl_6Cu$: C, H, N, Cu.

$[Cu(CCl_3COO)_2(caf)]_2$ (pale green form), (*3*): A solution of caffeine (1 mmol) in chloroform (10 ml) was added to a solution of $Cu(CCl_3COO)_2\cdot 3H_2O$ (1 mmol) in chloroform (20 ml) and 2,2-dimethoxypropane (1 ml). After the resulting solution had been concentrated to one-third of its volume, it was allowed to stand overnight at ca. 5 °C in a refrigerator. The pale green crystals were collected, washed with petroleum ether and dried *in vacuo* at room temperature. Anal. $C_{12}H_{10}N_4O_6Cl_6Cu$: C, H, N, Cu.

Magnetic measurements. Magnetic susceptibilities in the temperature range 80–300 K were determined by the Faraday method. The correction for diamagnetic contribution (χ_{dia}) was made by use of Pascal's constants.[5] The cryomagnetic data were fitted to the Bleaney–Bowers eqn. (1) allowing for the presence of paramagnetic impurity,[6] where P is the mole fraction of the monomeric copper(II) impurity, g_i is the average g factor for the impurity, and the other symbols have their usual meanings. The values $g_i = 2.2$ and $N\alpha = 60\times10^{-6}$ cgs emu were used throughout the present study. The best-fit parameters, $-2J$, g, and P, were obtained by using a non-linear least-

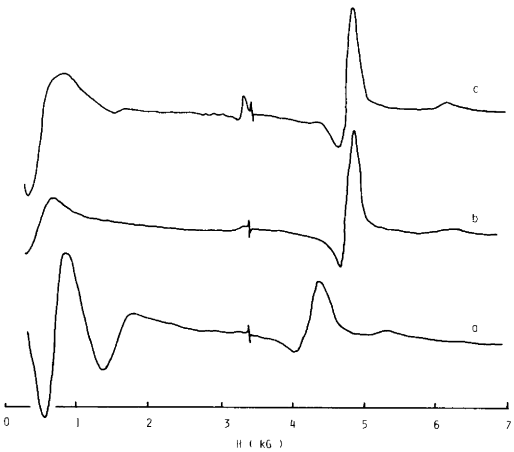

Fig. 5. Room temperature polycrystalline powder EPR spectra at X-band frequency. (a) Pale green form of $[Cu(CCl_3COO)_2(caf)]_2$, (*3*). (b) Light green form of $[Cu(CCl_3COO)_2(caf)]_2$, (*2*). (c) $[Cu(CCl_3COO)_2(caf)]_2\cdot(2bz)$, (*1*). The small features near 3.3 kG are due to monomeric Cu(II) impurities.

squares program, SALS (version D), written by T. Nakagawa (The University of Tokyo) and Y. Oyanagi (The University of Tsukuba), with a FACOM M-200 computer at the Nagoya University Computation Center. As a convenient statistical indicator of the quality of the least-squares fits, the discrepancy index, $\sigma_{dis} = [\Sigma(\chi_{obsd}-\chi_{calcd})^2/\Sigma\chi_{obsd}^2]^{1/2}$ was employed. The magnetic susceptibility data are presented in Tables 4–6 and shown in Figs. 3 and 4 as plots of χ_A vs. T. The values of $-2J$, g, P, and σ_{dis} are summarized in Table 7.

$$\chi = \frac{Ng^2\beta^2}{3kT}\left[1+\frac{1}{3}\exp\left(\frac{-2J}{kT}\right)\right]^{-1}(1-P) + \frac{Ng_i^2\beta^2}{4kT}P + N\alpha \quad (1)$$

EPR spectra. Polycrystalline powder EPR spectra were recorded on a Jeol JES-ME-2 spectrometer in the X-band range, and are shown in Figs. 5–7. The EPR parameters are given in Table 8.

X-ray crystallography. X-ray data were collected with an Enraf–Nonius CAD-4 automated diffractometer by Molecular Structure Corporation, College Station, Texas. A green, prismatic crystal of dicaffeinetetrakis(μ-trichloroacetato)dicopper(II) benzene solvate, (*1*), having approximate dimensions 0.50×0.20×0.15 mm was mounted on a glass fiber and Cu$K\alpha$ radiation was used for data collection. Cell constants were determined from setting angles of 25 reflections in the range $5<\theta<22°$. Based on systematic absences of hkl:$h+k = 2n+1$, the space group could be $C2$, Cm or $C2/m$ (Nos. 5, 8 or 12). Statistical tests indicated centrosymmetry. Intensities of 2564 unique reflections were collected out to $2\theta<140°$ using $\omega-2\theta$ scans, with scan rate 2 to 20° min^{-1} in ω, and with θ scan width = $(0.8+0.30\tan\theta)°$. Of the reflections collected, 460 had $I\leq0.5\sigma(I)$ and were discarded, as well as an additional 216 reflections with $F\leq\sigma(F)$. Three standard reflections were measured every 41 min. During data col-

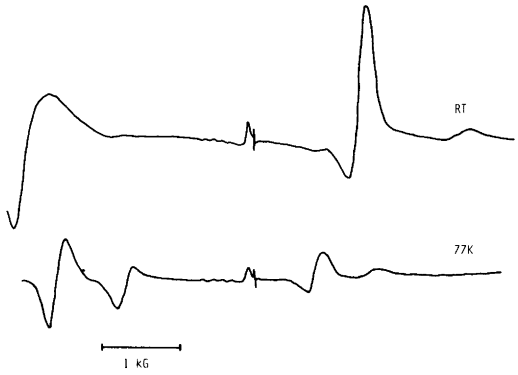

Fig. 6. X-band polycrystalline powder EPR spectra of the light green form of $[Cu(CCl_3COO)_2(caf)]_2$, (*2*), at room temperature (RT) and liquid nitrogen temperature (77 K). The small features near 3.3 kG are due to monomeric Cu(II) impurities.

Table 5. Magnetic susceptibilities[a] for $[Cu(CCl_3COO)_2(caf)]_2\cdot(2bz)$, (*1*). $\chi_{dia} = -326.9\times10^{-6}$ cgs emu.

T/K	$10^6\,\chi_A$
Low temp. region	
81.5	893.0
91.8	1031.6
102.3	1147.2
113.9	1256.3
129.7	1351.3
145.3	1410.4
154.1	1433.5
164.2	1441.2
174.3	1446.3
183.1	1442.5
196.2	1425.8
212.2	1402.7
230.1	1368.0
232.1	1368.0
235.1	1357.7
236.1	1356.4
237.0	1353.9
239.0	1350.0
Intermediate temp. region	
242.2	1330.8
244.2	1315.4
245.0	1301.2
248.0	1300.0
High temp. region	
250.1	1288.4
262.0	1249.9
280.0	1219.1
298.0	1181.8

[a] See footnote to Table 4.

Table 6. Magnetic susceptibilities[a] for $[Cu(CCl_3COO)_2(caf)]_2$, pale green form, (*3*). $\chi_{dia} = -272\times10^{-6}$ cgs emu.

T/K	$10^6\,\chi_A$
81.4	1758
88.3	1852
88.8	1861
91.0	1881
98.9	1949
105.7	1981
112.3	1996
117.7	2003
126.3	2003
138.2	1973
158.7	1894
181.9	1788
206.6	1679
230.0	1579
250.6	1499
275.1	1408
298.8	1321

[a]See footnote to Table 4.

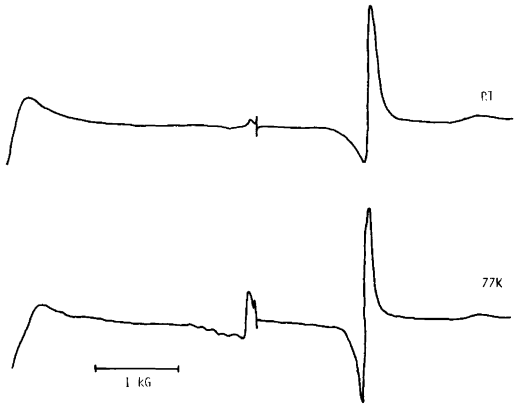

Fig. 7. X-band polycrystalline powder EPR spectra of $[Cu(CCl_3COO)_2(caf)]_2\cdot(2bz)$, (*1*), at room temperature (RT) and liquid nitrogen temperature (77 K). The small features near 3.3 kG are due to monomeric Cu (II) impurities.

lection, there was a loss in intensity for the three reflections of ca. 6%. A linear decay correction was therefore applied. Corrections were made for Lorentz, polarization and absorption effects (abs. corrn. empirical; min. transm. coeff. = 0.147, max. = 0.440). Programs used came from SHELX 76,[7] modified for a PDP 1144 computer.

The structure was solved by conventional heavy-atom methods and refined by successive experimentally weighted least-squares iterations assuming the correct space group to be *C2/m*. It soon became apparent that the trichloromethyl groups were disordered. This is, however, quite common for trihaloacetates.[4,8,9] A model with a main orientation of the three chlorines (occupancy 50%) and two other orientations (occ. 25% each) corresponding to rotations of ca. 35° and 20° around the C–CCl_3 bond (to each side of the main orientation) seemed to work best, and the successful refinement justified the choice of space group. Absence of high U_{22} values for Cu and for atoms in caffeine also supports the idea

Table 7. Magnetic data.

Compound	$-2J/cm^{-1}$	g	$P\times10^2$	$\sigma\times10^3$ [b]	$-2J/cm^{-1}$	g	$\sigma\times10^3$ [b]
(*1*)							
Low temp. region	202.7	2.265	4.58	1.57	184.6	2.216	14.5
High temp. region	–	–	–	–	194.5	2.223	3.87
(*2*)							
Low temp. region							
Sample A	177.5	2.421	2.85	2.71	169.2	2.388	5.34
Sample B	176.5	2.412	2.66	1.31	168.8	2.380	5.16
High temp. region							
Sample A	–	–	–	–	207.6	2.484	2.56
Sample B	–	–	–	–	200.6	2.452	1.82
(*3*)	135.7	2.222	1.88	1.54	–	–	–

[a]$N\alpha = 60\times10^{-6}$ cgs emu(fix.). [b]$N\alpha = 60\times10^{-6}$ cgs emu(fix.) and P=0(fix.)

Table 8. EPR parameters.

Compound	$g_{\|}$	$g_{\perp}$	g_{av}[a]	$\|D\|/cm^{-1}$	H_o/cm^{-1}
(*1*)					
Room temp.	2.488	2.142	2.263	.372	.316
77K	2.389	2.139	2.225	.220	.306
(*2*)					
Room temp.	2.468	2.109	2.235	.366	.316
77K	2.454	2.102	2.225	.367	.306
(*3*)					
Room temp.	2.317	2.143	2.203	.237	.316
77K	2.305	2.152	2.204	.223	.306

[a] $g_{av} = (1/3(g_{\|}^2+2g_{\perp}^2))^{1/2}$.

that those atoms lie on a mirror plane as required by *C2/m* (or *Cm*). Attempts at refinements in the alternative space groups gave no apparent improvement according to Hamilton's test.[10] Also, both the disorder in CCl_3 and the high symmetry of the dimer were found to persist in the noncentric space groups.

The hydrogen atoms were not included in the refinement. The other atoms were refined anisotropically, and refinement terminated when all parameter shifts were less than 0.06σ. The quantity minimized was $\Sigma w(F_o-F_c)^2$ where $w = 1/\sigma^2(F_o)$, $\sigma(F_o) = \sigma(I)/2F_o\mathrm{Lp}$ and $\sigma(I) = T(C+R^2B)^{1/2} + 0.005F_o^2$. T is the scan rate, R is the ratio of scan time to background counting time and B is the total background count. A final difference electron density map showed no maxima above 0.7 e^- $Å^{-3}$. Final $R = 0.068$, $R_w = 0.082$ and $S = 2.05$. Atomic coordinates are given in Table 1, interatomic distances and angles are listed in Table 2, and molecular planes are listed in Table 3.* Scattering factors used were taken from Cromer and Liberman,[11] Cromer and Mann[12] and Stewart, Davidson and Simpson.[13]

Results and discussion

Fig. 1 shows the structure of the dimer, $[Cu(CCl_3COO)_2\ (C_8H_{10}N_4O_2)]_2 \cdot 2C_6H_6$, (*1*). The benzene molecules as well as the chlorines are left out for the sake of clarity. With Z being 2, the space group symmetry requires the molecule to have *2/m* symmetry.

The Cu coordination. Each copper atom has a distorted, square pyramidal coordination sphere, with four coplanar oxygen atoms (Table 3) constituting the basal plane and N9 of the caffeine molecule at the apex. This is the standard conformation of $[Cu(RCOO)_2L]_2$ dimers.[14,15] Like other dimers, (*1*) has a short Cu---Cu contact *trans* to the Cu–L(N9) bond. While this contact is mostly in the range 2.56–2.67 Å in classical copper acetate dimers,[2,15] in (*1*), this distance is 2.852(2) Å and may be compared to 2.886(4), 2.766(3) and 2.732(av.) Å, the Cu–Cu distances found in the dimers with R = CF_3 and L = quinoline,[9] R = CCl_3 or CBr_3 and L = 2-chloropyridine,[1,16] and R = CCl_3 and L = benzonitrile,[3] respectively. Also, dimers with R = CH_2X (X=F,Cl) may have distances above 2.7 Å.[15] Earlier studies have shown that the Cu–Cu separation in such dimers increases with increasing strength of the parent bridging carboxylic acid.[17] Increasing Cu–Cu separation is known to be attended by increasing distance of Cu from the basal four-oxygen plane.[9,15] The present investigation provides no exception to that rule, with Cu being 0.32 Å above the plane. The Cu–N and average Cu–O bond lengths of 2.12(5) and 1.973 Å are normal.[15] Except for the chlorines, the bridging trichloroacetate ligands are nearly planar, with C1–O1 and C1–O2 being 1.215(5) and 1.245(5) Å, respectively. Also, the Cu–O–C1 angles are asymmet-

*Tables of observed and calculated structure factors, temperature factors and coordinates of the chlorine atoms with occupancy = 0.25 are available from the authors E.A.M. or S.H. upon request.

ric, being 127.7(4)° for O1 and 121.6(4) for O2. Angle O1–C1–O2 is 129.0(6)°. The literature reports a wide variation in these angles,[15] and the flexibility of such carboxylate bridges is considerable.[8]

The Cu′–Cu–N9 angle is only 163.4(3)°. This deviation from linearity is greater than that normally found in copper carboxylate dimers and is probably due to repulsion between the caffeine C13 methyl group on one side and Cu plus the Cl atoms of the bridging ligands (Cu---C13 = 3.56 Å and Cl3---C13 = 3.95 Å) on the other. This is also reflected in the large Cu–N9–C4 angle of 145.9(6)°, which is 13° greater than the corresponding angle found when a similar ligand, but with H instead of C13 methyl, is bonded to cobalt.[18] It may also be mentioned here that in the dichlorotriammine(caffeine)ruthenium(III) cation, such a repulsion (involving metal and C13 methyl) forces Ru to bind to the C8 atom of caffeine rather than to the expected site, N9.[19,20]

The caffeine ligand. Its structure is similar to those of free and protonated caffeines and similar purines.[19,21–26] The greatest differences are found in the five-membered ring. Compared to the most accurate caffeine structure,[22] the C5–N7 and C4–N9 bonds in (*1*) are 0.03 Å shorter and the N7–C8 and N9–C8 bonds are 0.03 and 0.07 Å longer. The angles also change, notably C4–N9–C8 which has the very low value of 102.0 (6)° in (*1*). All caffeine angles correspond to sp^2 hybridization of the ring atoms and the bond lengths indicate delocalized π bonding involving those atoms. The complete planarity of the ligand (except for methyl hydrogens) is not unexpected. Purine derivatives are nearly planar with C4–C5 twist angles of only a few degrees.[19,21–26] The caffeine ligands are staggered with respect to the Cu–O bonds.

Molecular packing. The benzene plays an important role in the packing of the molecules (Fig. 2). Each dimer may be viewed as consisting of a $Cu_2(CCl_3COO)_4$ box-like part with a flat caffeine part attached at each end. Since the dimer is centrosymmetric, the thickness of the box (in the *b* direction) is $b/2 \approx 7$ Å, roughly twice that of the caffeine part. Such a molecule is not easy to pack effectively and this may be the reason why the unsolvated dimer, (*2*), forms only a microcrystalline residue. However, in (*1*), the benzene molecules are stacked so that each caffeine ligand is sandwiched between two benzenes in the *b* direction, and vice versa. Since the benzenes are also located at centres of symmetry *b*/2 apart, the thickness of the caffeine ends of the dimer now effectively also becomes $b/2 \approx 7$ Å.

The stacking of the molecules in this manner is obviously quite effective. Since the benzenes are almost parallel with the caffeine ligands and the distance between the two are ca. 3.4–3.6 Å, there may be a weak charge-transfer interaction holding them together.

Magnetic properties. The phase transition temperature for $[Cu(CCl_3COO)_2(caf)]_2 \cdot (2bz)$, (*1*), ca. 245 K, is higher by about 25 K than that for the light green form of $[Cu(CCl_3COO)_2(caf)]_2$, (*2*). The variable-temperature magnetic susceptibilities for low and high temperature regions of these complexes in Tables 4 and 5 are well reproduced by eqn. (1). In order to make sure that the observed phase transition in these complexes is real, magnetic measurements were made on two samples (A and B) of (*2*) (Table 4 and Fig. 3). In the low temperature region, the magnetic parameters obtained for the two samples coincided well, indicating that the observed novel transition of the caffeine adducts is genuine (Table 7). In the high temperature region, however, least-squares fittings with significant results were obtained only by setting $P=0$ in eqn. (1). This is presumably due to the fact that fewer susceptibility data were collected in this region as compared to the low temperature region. As is seen from Table 7, setting $P=0$ tends to decrease the values of $-2J$ and g. Comparison of the magnetism of these complexes in the low and high temperature regions should therefore be made only with the parameters obtained by setting $P=0$. The low temperature $-2J$ value for (*1*) was somewhat larger than that for (*2*), while in the high temperature region, a lower $-2J$ value was observed for (*1*). The $-2J$ value for the pale green form of (caf) adduct, (*3*), 135 cm^{-1}, is quite small compared with those of (*1*) and (*2*). The EPR spectral features of (*3*) are quite different from the room temperature spectra of (*1*) and (*2*) (Fig. 5). They are fundamentally the same as those observed for $[Cu(CPh_3COO)_2(py)]_2 \cdot (bz)$: ($-2J$ = 184 cm^{-1}, Cu–Cu = 3.086 Å), whose structure has recently been determined by Steward *et al.* and found to have a trigonal-bipyramidal metal geometry.[27]

For these two complexes, an unfamiliar relation, $D<H_0$, was observed,[27-29] and this relation has been revealed for a number of copper(II) trichloroacetate adducts whose $-2J$ values are quite small compared with those of the common copper(II) carboxylates ($-2J \approx 300\ cm^{-1}$)[30] which have square-pyramidal metal geometry and obey the common relation $D>H_0$.[31] Stepwise variable-temperature EPR measurements on (*2*) were repeated between room temperature and liquid nitrogen temperature. However, no particular spectral change could be detected between the two extreme temperatures (Fig. 6). On the other hand, the EPR spectral features of (*1*) at liquid nitrogen temperature were quite different from those at room temperature (Fig. 7): The low-temperature EPR spectrum appears to be essentially the same as the room-temperature EPR spectrum of (*3*) accompanying the uncommon relation, $D<H_0$ (Table 8). The spectral interconversion accompanied by $D \gtrless H_0$ thus takes place reversibly. This interesting finding prompted us to attempt a low-temperature structural study of (*1*). However, the crystals cracked upon cooling and were thus rendered unsuitable for an X-ray crystallographic investigation. From the magnetic data above it may be speculated that the structure of (*3*) perhaps has the copper atoms in a trigonal-bipyramidal environment, and from the EPR data one may guess at the possibility of such an environment also for the low-temperature form of (*1*). The *g* values obtained by EPR are smaller than those obtained by the magnetic susceptibility measurements (Tables 7 and 8). This is often observed for copper(II) carboxylate dimers.[32]

Acknowledgements. Support for this investigation by the Robert A. Welch Foundation of Houston, Texas, the Norwegian Research Council for Science and the Humanities, and the National Science Foundation, USA (INT-8217957), is gratefully acknowledged.

References

1. Moreland, J. A. and Doedens, R. J. *Inorg. Chem. 17* (1978) 674.
2. Rao, V. M., Sathyanarayana, D. N. and Manohar, H. *J. Chem. Soc. Dalton Trans.* (1983) 2167.
3. Nakashima, M., Mikuriya, M. and Muto, Y. *Bull. Chem. Soc. Jpn. 58* (1985) 968.
4. Porter, L. C., Dickman, M. H. and Doedens, R. J. *Inorg. Chem. 22* (1983) 1962.
5. Selwood, P. W. *Magnetochemistry,* Interscience Publishers, New York 1956, pp. 78 and 91.
6. Ginsberg, A. P. *Inorg. Chem. Acta Rev. 5* (1971) 45.
7. Sheldrick, G. M. *SHELX 76. A Program for Crystal Structure Determination,* University of Cambridge, England 1976.
8. Porter, L. C. and Doedens, R. J. *Inorg. Chem. 24* (1985) 1006.
9. Moreland, J. A. and Doedens, R. J. *J. Am. Chem. Soc. 97* (1975) 508.
10. Hamilton, W. C. *Acta Crystallogr. 18* (1965) 502.
11. Cromer, D. T. and Liberman, D. *J. Chem. Phys. 53* (1970) 1891.
12. Cromer, D. T. and Mann, J. B. *Acta Crystallogr. Sect. A 24* (1968) 321.
13. Stewart, R. F., Davidson, E. R. and Simpson, W. T. *J. Chem. Phys. 42* (1965) 3175.
14. Kato, M., Jonassen, H. B. and Fanning, J. C. *Chem. Rev. 64* (1964) 99.
15. Melnik, M. *Coord. Chem. Rev. 42* (1982) 259.
16. Porter, L. C. and Doedens, R. J. *Inorg. Chem. 23* (1984) 997.
17. Melnik, M. *Coord. Chem. Rev. 36* (1981) 1.
18. Marzilli, L. G., Epps, L. A., Sorrell, T. and Kistenmacher, T. J. *J. Am. Chem. Soc. 97* (1975) 3351.
19. Krentzien, H. J., Clarke, M. J. and Taube, H. *Bioinorg. Chem. 4* (1975) 143.
20. Hodgson, P. J. *Prog. Inorg. Chem. 23* (1977) 211.
21. Sutor, D. J. *Acta Crystallogr. 11* (1958) 453.
22. Shefter, E. *J. Pharm. Sci. 57* (1968) 1163.
23. Mercer, A. and Trotter, J. *Acta Crystallogr. Sect. B 34* (1978) 450.
24. Kistenmacher, T. J. and Sorrell, T. *Acta Crystallogr. Sect. B 31* (1975) 489.
25. Thiessen, W. E., Levy, H. A. and Flaig, B. D. *Acta Crystallogr. Sect. B 34* (1978) 2495.
26. Nakao, S., Fujii, S., Sakaki, T. and Tomita, K.-I. *Acta Crystallogr. Sect. B 33* (1977) 1373.
27. Steward, O. W., Kato, M., Chang, S. C., Sax, M., Chang, C. H., Taura, T., Jury, C. F., Muto, Y., Tokii, T., Pletcher, J. and Yoo, C. S. *Proc. 23rd Int. Conf. Coord. Chem.,* Boulder, CO, USA, July 29 – August 3, 1984, p. 247.
28. Kato, M., Taura, T., Steward, O. W., Tokii, T., Muto, Y., Kushi, Y. and Suzuki, I. *Proc. 33rd Conf. Coord. Chem. Chem. Soc. Jpn.,* Toyonaka, Japan, October 1983, p. 494.

29. Price, J. H., Pilbrow, J. R., Murray, K. S. and Smith, T. D. *J. Chem. Soc. A* (1970) 968.
30. Horie, H., Nakashima, M., Tokii, T., Muto, Y., Kato, M. and Suzuki, I. *Proc. 33rd Conf. Coord. Chem. Chem. Soc. Jpn.* Nagaoka, Japan, October 1983, p. 476.
31. Wasson, J. R., Shyr, C.-I. and Trapp, C. *Inorg. Chem. 7* (1968) 469.
32. Muto, Y. *et al. Unpublished data*; Erre, L. S., Micera, G., Piu, P., Cariati, F. and Ciani, G. *Inorg. Chem. 24* (1985) 2297.

Received May 26, 1986.